DE GRUYTER OPEN

Acta Geophysica
vol. 64, No. 4, Aug. 2016, pp. 1164-1175
DOI: 10.1515/acgeo-2016-0040

The Influence of a Local Fault Zone on High Energy Tremor Occurrence During Longwall Mining of a Coal Seam

Łukasz WOJTECKI[1], Małgorzata KNOPIK[2], and Wacław Marian ZUBEREK[2]

[1]Kompania Węglowa S.A., Katowice, Poland; e-mail: l.wojtecki@kwsa.pl

[2]University of Silesia in Katowice, Faculty of Earth Sciences, Sosnowiec, Poland; e-mail: gosia_knopik@interia.pl, waclaw.zuberek@us.edu.pl

Abstract

Underground mining of coal seams in the Upper Silesian Coal Basin in Poland is accompanied by seismic activity of varying magnitude. The investigations which have been performed for several years distinguished high energy mine tremors connected directly with mining or coupled with geological structures, such as large faults. In mined seams, local fault zones occur. Faults in these zones are usually small, with throws comparable with coal seams thicknesses. Local fault zone may be responsible for the occurrence of high energy tremors as well as large faults, as presented in this article. An analysis of source mechanism of high energy tremors generated during longwall mining of the coal seam No. 510, with presence of a local fault zone, in one of the Polish hard coal mines in the Upper Silesian Coal Basin was performed. For this purpose, the seismic moment tensor inversion method was used. In most of foci, the process of shear predominated. Determined nodal plane parameters were correlated with parameters of faults forming the local fault zone. High energy tremors were generated mostly by dislocations on faults of the local fault zone. Weakening of roof rocks in the neighborhood of local fault zone takes an important role too, and was responsible for share of implosion in the focal mechanism.

Key words: mine tremors, focal mechanism, seismic moment tensor, underground coal mining.

1. INTRODUCTION

Underground mining of coal seams in the Upper Silesian Coal Basin generates mine tremors, including those with high energy. These tremors may be correlated with mining operation and their energy is adequate to specific geological and mining conditions. Some tremors are coupled to geological structures, such as large faults.

An analysis of the tremor source mechanism allows to reconstruct the way of rock mass destruction in the focal zone. The most probable factors affecting the generation of seismic events may be determined. The determination of mechanisms which are responsible for the occurrence of mine tremors is possible with the use of seismic moment tensor inversion method. This method was firstly used in global seismology, and next was adapted to mine tremors analysis (Gibowicz and Kijko 1994, Marcak and Zuberek 1994, Gibowicz 1995, Stec 2009, Kwiatek 2009, Stec and Wojtecki 2011).

The method of seismic moment tensor inversion was applied for determination of source mechanisms of high energy tremors induced during mining of coal seam No. 510 in one of the coal mines in the Upper Silesian Coal Basin, in a certain time interval. The most probable ways of generation of these tremors were defined. The results of the analysis have been compared with local geological and mining conditions.

The presented analyses were performed to determine the factors responsible for the occurrence of high energy tremors during longwall mining under complicated geological and mining conditions. Understanding the processes which take place in the tremors' foci (especially those with high energy) enables a proper assessment of the rockburst hazard in coal mines with the use of seismological method and application of adequate prevention. The local fault zone was the main factor influencing the high energy tremor occurrence. This knowledge was applied for determination of rockburst prevention methods in the longwall and will be also useful for seismicity forecast during planning of further longwall mining.

2. GEOLOGICAL AND MINING CONDITIONS

The coal seam No. 510 in the area of the longwall was deposited at a depth of about –835 to –910 m and its thickness varied from 5.3 to 8.1 m. The smallest thickness of the coal seam was correlated with the local fault zone occurrence.

In the floor of the coal seam No. 510, shale, sandy shale, and fine-grained sandstone are deposited. Sandy shale, fine-grained sandstone, another sandy shale, and shale occur in the roof of the coal seam No. 510. The total thickness of these layers is lower than 13 m. The floor of coal seam No. 507 is above. At a distance of more than 70 m above the seam No. 510,

a thick layer of sandstone is deposited. This sandstone has high value of uniaxial compressive strength (up to 80 MPa), and its maximum thickness – with some thin layers of shales and sandy shales – is 60 m.

The longwall with caving was running in the upper layer of coal seam No. 510, from west to east. The longwall advance in the following months (from November 2012 to December 2013) is shown in Fig. 1 (the bold line represents the location of longwall face at the beginning). The longwall started from neighborhood of pillar for flank drifts, in a short distance from large fault, which has strike NW-SE and throw $h = 25$ m (Fig. 1). Mining under the above-mentioned conditions was responsible for the occurrence of high energy tremors (Knopik *et al.* 2015). High energy tremors have seismic energy $E \geq 1 \times 10^5$ J (magnitude $M_L \geq 1.68$). The longwall was running along the gob created in the upper stage (Fig. 1).

In the area of the longwall, the local fault zone occurred. This zone consisted of several faults, with strikes from SW-NE to WNW-ESE, throws from $h = 0.2$ to 5.5 m, and dips from near 20° to near 90° (generally SE, but S and NW as well). The location of local fault zone and values of throws and dips of faults forming this zone are shown in Fig. 1.

In the longwall area, coal seam No. 507 has been mined several years ago. The longwall in the wholeness was running under the gob created in coal seam No. 507. Coal seam No. 502, deposited at a distance of about 126 m above coal seam No. 510, has been mined still earlier. However, the longwall was running under the mining remnant of irregular shape in coal seam No. 501 (Fig. 1), deposited at a distance of about 140 m above coal seam No. 510. This mining remnant was responsible for the observed increase of stress in rock mass, during running of the longwall.

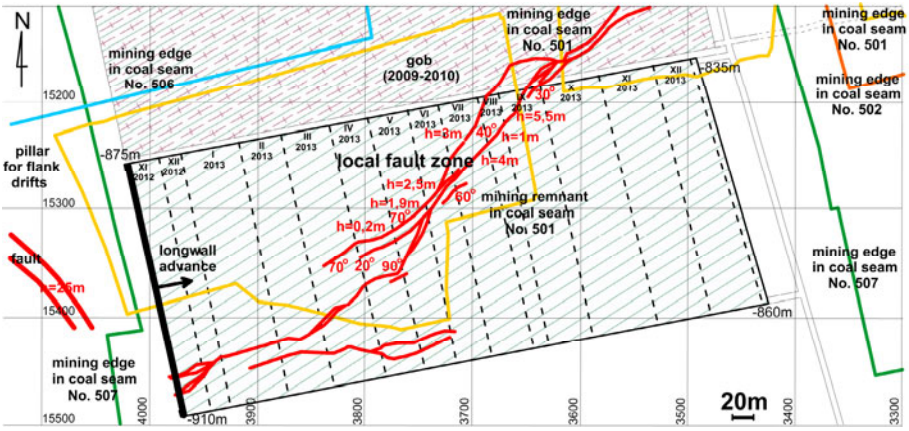

Fig. 1. The longwall area on the coal seam No. 510 map.

3. HIGH ENERGY TREMORS IN THE AREA OF LONGWALL

Mining of coal seam No. 510 with the longwall lasted nearly 14 months (from November 2012 to December 2013). High energy tremors accompanied this longwall mining, which indicated a high level of rockburst hazard. Total number of recorded high energy tremors was 61 with magnitude M_L from 1.84 to 2.74. According to seismic activity, correlated to geological and mining conditions, running of the longwall could be divided into two periods.

During the first 6 months, the longwall run away from the neighbourhood of protecting pillar for flank drifts and large fault (throw $h = 25$ m). During this period, 28 high energy tremors occurred with magnitude M_L from 1.84 to 2.74. High energy tremors in this period were caused by a change of stress equilibrium in the pillar for flank drifts and dislocations on large fault (Knopik *et al.* 2015). Some of high energy tremors were caused also by cracking of thick layer of sandstone above mined coal seam and destruction of roof rocks because of gob formation (Knopik *et al.* 2015). In this period, the total longwall advance equalled 225 m.

The second period lasted nearly 8 months. During the first four months of this period the longwall was running through the local fault zone, where the roof was weak. Keeping the stabilization of the roof affected the longwall advance, which equalled only 121 m. During the last four months the roof in the area of the longwall was tougher, which allowed to get longwall advance of 194 m. During the second period, 33 high energy tremors occurred with magnitude M_L from 1.84 to 2.58. Hypocentres of these tremors were localized behind the longwall, mainly in the local fault zone or its direct neighbourhood (with an average error of epicentre location amounting to 20 m). In the area of the longwall, the maximum error of epicentre location achieved about 35 m, and it depended on the seismic stations which had been taken into calculations (Kołodziejczyk 2009). The error of hypocentre location in the area of the longwall was larger and in extreme cases reached over 60 m (Kołodziejczyk 2009). Focal mechanisms of these tremors were determined.

4. CALCULATION OF THE FOCAL MECHANISM

Focal mechanism of mine tremors could be calculated with the use of seismic moment tensor inversion method. In this method, the seismic moment tensor components are calculated on the basis of displacement field recorded by seismic network surrounding the source. Displacements at a long distance from the seismic source are a sum of displacements caused by each of force couples (Aki and Richards 1980). The tensor decomposition into the isotropic component (I), the compensated linear vector dipole (CLVD), and a

double couple of forces (DC) is the most often used characterization of the focus of mine tremor (Gibowicz and Kijko 1994, Marcak and Zuberek 1994, Gibowicz 1995, Stec 2009). The isotropic part I describes the volumetric changes in the source ("+" means explosion, "–" means implosion), CLVD describes a mechanism similar to the uniaxial compression ("–") or tension ("+") and DC relates to shear mechanism. The advantage of the isotropic part in full seismic moment tensor concerns tremors generated because of roof weight on coal seam causing the exceedance of its compressive strength (explosive mechanism) or a collapse of roof rocks into cavern caused by mining (implosive mechanism). The compensated linear vector dipole (CLVD) describes cracking of pillars. The advantage of the double couple of forces (DC) indicates sliding of rock masses (Gibowicz and Kijko 1994), for example by activation of faults presented in rock mass.

Focal mechanisms were calculated by the seismic moment tensor inversion based on the analysis of seismic waves generated in the focus and registered by the underground seismic stations surrounding the source. The data set has been obtained from a network of 16 seismic stations, located in underground excavations at depths from 320 to 1000 m below the sea level. The network is composed of vertical SPI-70 seismometers and DLM-2001 geophones installed on bolts and oriented vertically. These sensors measure signals having a frequency from 1 Hz. The upper limit of transmitted frequencies is 50 Hz. Signals are recorded with dynamic range less than 72 dB. Each channel has its own amplitude gain. The sampling rate is 5000 samples per second. The timing of seismological system is synchronized by Global Positioning System.

Seismic moment tensor calculation was performed in the FOCI software (Kwiatek 2009), based on an inversion of *P*-wave amplitude, taking into account the directions of the first deflection in the time domain (Stec and Wojtecki 2011).

Mechanisms of all 33 events that occurred in the second period of mining, mostly in the local fault zone or its neighbourhood, have been estimated. Focal mechanisms were determined on the basis of records registered by seismological network of hard coal mine. For seismic moment tensor determination, 14 or 15 records were used most often (about 64 and 18% of tremors, respectively). The minimal number of records taken into account was 12 (about 6% of tremors). Seismic stations were distributed evenly and optimally around the longwall (Fig. 2). Squares with "S" in Fig. 2 represent seismic stations.

The calculations were made using L1 norm, because of its lower sensitivity to possible large errors, caused, for example, by random noise made by mining machines. Vertical coordinates of focus were improved by the FOCI software (Kwiatek 2009), testing the seismic moment tensor solution and as-

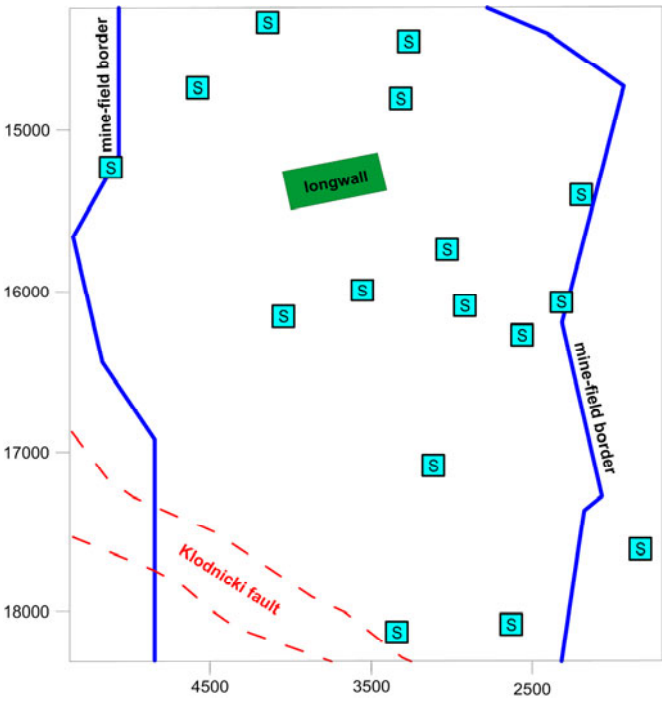

Fig. 2. Configuration of the seismic network around the longwall in coal seam No. 510.

suming the value corresponding to the highest values of quality coefficient (from 29 to 49%, mean 38%) – taking into consideration configuration of seismic stations and error of result – and the smallest error of estimation. Relative error of calculated seismic moments was 3% on average.

5. RESULTS

Results of the focal mechanism analysis of tremors recorded during second period of the longwall run are presented in Table 1. The criteria of focal mechanism types were specified by authors. If the share of DC component in full seismic moment tensor solution equals 50% or more, focal mechanism type is classified as normal (NO) or reverse (RE) slip mechanism. The only exception to this criterion is a focal mechanism type (RE) of tremor No. 5 (Table 1), where the share of DC component equals almost 50%, the share of uniaxial compression is higher than 40%, and the implosion practically does not matter (Table 1). For the other tremors, if the share of implosion is higher than 40%, the focal mechanism type is classified as IMPL. Some mixed types of focal mechanism, which do not satisfy the above mentioned

Table 1

Seismological and focal mechanism parameters of high energy tremors occurred during mining of coal seam No. 510 with the longwall

No.	Date	Time		M_L	Z[1)] [m]	Nodal planes parameters[2)]		Components of full seismic moment tensor [%]			Type mechanism
		h	m			ΦA/δA λA	ΦB/δB λB	I	CLVD	DC	
1.	18 Jun 2013	3	17	2.05	–825	19.7°/86.5° 116.2°	116.8°/26.4° 7.9°	–22.2	–20.8	57	RE
2.	28 Jun 2013	18	11	2.00	–809	18°/75.4° 111.6°	140.4°/25.9° 35.2°	–4.7	–6.1	89.3	RE
3.	8 Jul 2013	4	45	2.13	–829	230°/87.6° –115.8°	135.1°/25.9° –5.5°	–9.4	–18.4	72.2	NO
4.	22 Jul 2013	22	29	2.37	–829	219.6°/87.8° –115.3°	125°/25.4° –5.1°	–23.2	–24.1	52.8	NO
5.	27 Jul 2013	7	9	2.00	–829	43.2°/86.5° 107.2°	144.3°/17.5° 11.7°	–11.8	–40.7	47.4	RE
6.	2 Aug 2013	17	21	2.16	–822	217.8°/85.8° –117.2°	119.7°/27.5° –9.2°	–24.5	–15.4	60.1	NO
7.	14 Aug 2013	13	39	2.09	–801	212.4°/81.6° –113.8°	104°/25.1° –20.2°	–34.4	–30.8	34.8	NO/IMPL
8.	18 Aug 2013	9	28	2.19	–820	223.8°/67.3° –114.3°	93.3°/32.8° –45.4°	–42.3	–36.5	21.2	IMPL
9.	20 Aug 2013	20	9	2.19	–820	228.2°/72.9° –113.9°	104.6°/29° –37.2°	–34.9	–25.3	39.8	NO/IMPL
10.	23 Aug 2013	4	22	2.19	–810	254°/76.1° –107.5°	126.8°/22.2° –39.4°	–15.3	–1.8	82.9	NO
11.	26 Aug 2013	22	1	2.46	–829	231.8°/73.3° –113.5°	108.4°/28.5° –36.9°	–32.1	–16.3	51.6	NO
12.	31 Aug 2013	8	31	2.21	–827	230.8°/70.5° –114.1°	104°/30.7° –41°	–36	–22.9	41.1	NO/IMPL
13.	6 Sep 2013	8	25	2.37	–827	224.5°/78.5° –116.1°	112.4°/28.3° –24.8°	–32.3	–32.4	35.3	NO/IMPL
14.	11 Sep 2013	11	19	1.84	–824	225.9°/77.7° –117.4°	113.6°/29.9° –25.4°	–31	–13.8	55.2	NO
15.	20 Sep 2013	0	38	2.16	–821	245.5°/65.3° –110.6°	104.5°/31.8° –52.6°	–37	–23.5	39.5	NO/IMPL
16.	23 Sep 2013	17	40	2.05	–827	48.5°/69.2° 115.1°	175.5°/32.2° 41.7°	24.8	23.5	51.8	RE
17.	30 Sep 2013	15	21	2.19	–823	249°/61.4° –106°	99.9°/32.4° –63.2°	–36.9	–21.3	41.8	NO/IMPL

to be continued

Table 1 continuation

No.	Date	Time		M_L	$Z^{1)}$ [m]	Nodal planes parameters[2)]		Components of full seismic moment tensor [%]			Type mechanism
		h	m			ΦA/δA λA	ΦB/δB λB	I	CLVD	DC	
19.	8 Oct 2013	3	3	1.84	–828	242.3°/60.4° –113.7°	104°/37.2° –54.7°	–41.9	–31.2	27	IMPL
20.	9 Oct 2013	21	18	2.05	–827	237.8°/55.8° –111.4°	92.8°/39.6° –61.7°	–45.1	–39.5	15.4	IMPL
21.	15 Oct 2013	7	17	2.05	–825	245.8°/59.9° –110.2°	102.1°/35.7° –59.2°	–41.3	–31.2	27.5	IMPL
22.	16 Oct 2013	16	31	2.05	–800	235.6°/64.2° –115.9°	103.7°/35.9° –47.9°	–40.6	–26.7	32.7	IMPL
23.	18 Oct 2013	17	14	2.21	–830	235°/74° –114.7°	114°/29.2° –34.5°	–32.7	–18.5	48.8	NO/IMPL
24.	23 Oct 2013	20	34	2.05	–825	256.6°/54.6° –125.5°	127.5°/48.4° –50.8°	–35	–39.4	25.6	IMPL/NO
25.	30 Oct 2013	23	53	2.00	–818	249.6°/61.9° –104.1°	97.7°/31.2° –65.5°	–37.7	–21.8	40.5	NO/IMPL
26.	6 Nov 2013	12	5	2.37	–808	250.6°/67° –108.7°	111.6°/29.4° –52.9°	–32.1	–17.1	50.7	NO
27.	15 Nov 2013	4	39	2.00	–804	254.1°/57.2° –108.9°	106.5°/37.3° –63.6°	–41	–19.3	39.7	IMPL
28.	23 Nov 2013	1	4	2.58	–720	19.2°/65.2° –70.9°	159.6°/31° –125.3°	–21.3	–18.6	60.1	NO
29.	30 Nov 2013	12	5	2.05	–703	23.4°/68.4° –69.8°	158.5°/29.3° –131°	–25.6	–24.5	50	NO
30.	11 Dec 2013	9	55	2.05	–815	274.5°/47.1° –77.3°	76.2°/44.4° –103.3°	–39.5	–14.4	46.1	NO/IMPL
31.	14 Dec 2013	2	12	2.37	–772	148.2°/73.2° 79°	2.2°/20° 122.4°	27.6	22.1	50.2	RE
32.	21 Dec 2013	23	16	2.05	–816	156.8°/53.1° 59.2°	21.6°/46.6° 124.3°	21	18.8	60.2	RE
33.	4 Jan 2014	14	20	2.00	–782	246.3°/67° –114.2°	115.2°/32.9° –46°	–34.9	–15.5	49.6	NO/IMPL

[1)]focus depth from the best fitting solution by the FOCI software, [2)]nodal plane parameters: ΦA, ΦB – azimuth of nodal planes A, B; δA, δB – dip of nodal planes A, B; λA, λB – rake angle correlated with nodal planes A, B.

criteria, occur too. If the normal slip mechanism dominates the implosion, such a mechanism is classified as NO/IMPL; otherwise, the focal mechanism is classified as IMPL/NO.

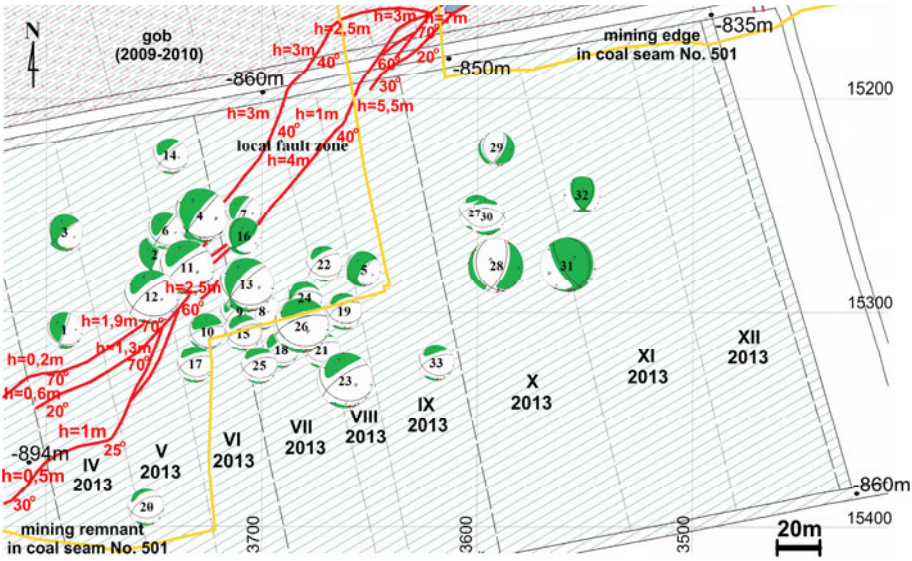

Fig. 3. Location of epicentres and focal mechanisms of analyzed high energy tremors on the coal seam No. 510 map.

Solutions of focal mechanism of all analyzed tremors are graphically presented in Fig. 3 with the use of focal spheres. The equal-area projection (Schmidt's projection) on the lower hemisphere was used. In each sphere the green area represents tension, and the white area – compression. Inside every focal sphere the ordinal number of tremor is included. Small-sized spheres represent tremors with energy of the order of 10^5 J (magnitude $1.68 \leq M_L < 2.21$). Large-sized spheres represent tremors with energy of the order of 10^6 J ($2.21 \leq M_L < 2.74$).

In focal mechanisms of near 45.5% of tremors (15 cases) shear mechanism predominated (tremors Nos. 1-6, 10, 11, 14, 16, 26, 28, 29, 31, 32). The DC component achieved maximally 89.3% (mean 59.4%). Participation of other components was lower: the isotropic component varied from 4.7 to 32.1% (mean 21.8%), and the CLVD component ranged from 1.8 to 40.7% (mean 18.8%).

The normal slip mechanism occurred in 60% of tremors' foci with shear component domination (9 cases). An azimuth of one of the nodal planes in 78% of foci with normal slip mechanism ranged from 217.8° to 254° (mean 232.8°), and a dip angle ranged from 67°NW to 87.8°NW (mean 79.3°NW), which is clearly correlated with the local fault zone parameters (Fig. 3). In the foci of tremors Nos. 28 and 29 an azimuth of one of nodal planes equaled 159.6° and 158.5°, which was quasi parallel to the face position of the

longwall. A dip angle of these nodal planes was 31°W and 29.3°W. These tremors occurred after longwall had left the local fault zone (Fig. 3). Displacement of rock mass in these foci was most probably in the direction of gob and local fault zone. The best solutions of seismic moment tensor inversion were achieved for depths of –720 and –703 m, which clearly corresponds to cracking of thick layer of sandstone above the coal seam.

The reverse slip mechanism occurred in 40% of foci with shear component domination (6 cases, including tremor No. 5). An azimuth of one of nodal planes in these foci ranged from 116.8° to 175.5° (mean 147°), which was quasi parallel to the position of longwall face. Dip angles of these nodal planes for the four tremors (Nos. 1, 2, 5, 16) ranged from 17.5°E to 32.2°E (mean 25.5°E), which indicates shallow (near horizontal) reverse thrust faulting in roof-rocks. In foci of tremors Nos. 31 and 32 (Fig. 3), which occurred when the longwall has almost finished, the reverse slip mechanism also occurred, but dip angles of the above-mentioned nodal planes were larger, amounting to 73.2°E and 53.1°E, respectively. The reverse slip mechanism occurs when the horizontal compressive stresses and the vertical tensile stresses dominate together. At a large depth, compressive stresses in rock mass occur naturally. The level of compressive stress is particularly high near the longwall face. Probably rock mass destruction in the area of the local fault zone and large subsidence caused deflection of the layers of tough rocks (sandstones) deposited above, in which the additional vertical tensile stresses appeared. These conditions were responsible for reverse slip mechanism in foci of tremors Nos. 1, 2, 5, 16, 31, and 32.

In foci of nearly 33.3% of tremors – 11 cases (tremors Nos. 7, 9, 12, 13, 15, 17, 18, 23, 25, 30, 33) − the participation of shear component was insignificantly higher than implosion (near 6.2% on average). CLVD component had a lower share (mean 22.6%). Taking into account only the DC component, occurrence of these tremors corresponded with the local fault zone. In these foci the normal slip mechanism occurred (Fig. 3). An azimuth of one of nodal planes ranged from 212.4° to 274.5° (mean 238.7°), and a dip angle ranged from 47.1°NW to 81.6°NW (mean 68.3°NW), which is connected with local fault zone parameters. Participation of implosion was important too. Because of weak roof, the caving process took place largely.

In foci of nearly 21.2% of tremors – 7 cases (tremors Nos. 8, 19-22, 24, 27) − an implosion dominated (Fig. 3). In 6 cases this domination was clear (share of implosion was higher than 40%). In focal mechanism of tremor No. 24 the share of implosion equaled 35%. In full seismic moment tensor solution the I component equaled, on average, 41%, and the CLVD and DC components were 32 and 27% on average, respectively. Taking into account only the DC component, the considered tremors were in some way correlated with local fault zone. An azimuth of one of nodal planes ranged from

223.8° to 256.6° (mean 242.3°), and a dip angle ranged from 54.6°NW to 67.3°NW (mean 59.9°NW), which is well correlated with local fault zone parameters. However, the collapse of weak roof rocks in the area of the local fault zone was the main factor responsible for these tremors occurrence. Stress level coming from mining remnant of coal seam No. 501 was probably also of importance.

6. DISCUSSION AND SUMMARY

Focal mechanisms of 33 high energy mine tremors (with magnitudes between 1.84 and 2.58), recorded by mine seismic network during longwall mining of coal seam No. 510 in one of the USCB coal mines, have been determined. Determination of focal mechanism supported the information about factors responsible for the occurrence of analyzed tremors.

Among geological and mining factors, an activation of local fault zone contributed to the highest degree to high energy tremors occurrence. In the source mechanism of analyzed mine tremors, the shear component clearly or insignificantly predominated. The roof rocks' weakening in the neighborhood of local fault zone was significant too. The collapse of roof rocks was reflected in great share of implosion in the full solution of seismic moment tensor. In some foci, an implosion even predominated. Taking into account only the DC part of full solution of seismic moment tensor of the abovementioned tremors, the calculated nodal plane parameters: azimuth (mean 238°) and dip (mean 69°NW) corresponded to the parameters of local fault zone. In the area where foci of analyzed tremors were concentrated, faults forming the local fault zone had strikes from 210° to 240° (calculated in the same way as the nodal plane azimuth) and dips between 60°SE and 70°SE. A difference between the calculated azimuth and dip of nodal planes and average strike and dip of faults forming the local fault zone were 15° and 9° on average, respectively. Some tremors occurred due to cracking of a thick layer of sandstone (normal or reverse slip mechanism).

Occurrence of high-energy tremors was clearly correlated with the local fault zone. This zone was a factor influencing on the level of rockburst hazard during mining of coal seam No. 510 with selected longwall.

Knowing the reason of the occurrence of high energy tremors, appropriate preventive measures were applied for improving the safety of mining. A restriction of crew movement was applied and a lining of galleries was reinforced. Some blastings in coal seam No. 510 were performed to minimize the risk of coal bump, which might be initiated by high energy tremors.

The results obtained will be helpful during planning of further longwall mining in the assigned underground coal mine. On this basis, rockburst prevention methods and parameters of longwall lining will be established.

References

Aki, K., and P.G. Richards (1980), *Quantitative Seismology – Theory and Methods*, Vols. 1, 2, W.H. Freeman & Co., San Francisco.

Gibowicz, S.J. (1995), Mechanism of tremor foci, mining tremors – mechanism, location and energy. **In:** *Proc. School of Underground Mining, 27 February – 3 March 1995, Szczyrk, Poland*, 5-30 (in Polish).

Gibowicz, S.J., and A. Kijko (1994), *An Introduction to Mining Seismology*, Academic Press, San Diego.

Knopik, M., W.M. Zuberek, and Ł. Wojtecki (2015), Multisources of high-energy mine tremors occuring during longwall mining of coal seam in varied geological and mining conditions, *Prz. Górn*. **12**, 12-19 (in Polish).

Kołodziejczyk, P. (2009), Optimization of the seismic network in Kompania Węglowa S.A., Tech. Report, SITG, Gliwice (in Polish, unpublished).

Kwiatek, G. (2009), Foci-seismic moment tensor – spectral parameters: A description of the program, available from: http://induced.pl/foci.

Marcak, H., and W.M. Zuberek (1994), *Mining Geophysics*, Śląskie Wydawnictwo Techniczne, Katowice (in Polish).

Stec, K. (2009), The focal mechanism and the methods of its calculation. **In:** *Workshop of the "Natural Hazards in the Mining Industry", 17-19 June 2009, Bogatynia-Świeradów Zdrój, Poland*, 287-305 (in Polish).

Stec, K., and Ł. Wojtecki (2011), Characteristics of the mine tremor source mechanism associated with the mining in the seam 510, the longwall 502 in the "Bielszowice" Coal Mine, *Res. Rep. Centr. Min. Inst.: Min. Environ.* **1**, 61-77 (in Polish).

Received 13 November 2014
Received in revised form 6 August 2015
Accepted 18 August 2015